Author Manuscript

Author Manuscript

Author Manuscript

Author Manuscript

HHS Public Access

Author manuscript

Neuroscience. Author manuscript; available in PMC 2021 November 21.

Published in final edited form as:

Neuroscience. 2020 November 21; 449: 214–227. doi:10.1016/j.neuroscience.2020.09.043.

Mechanisms Underlying Neuroplasticity in the Nucleus Tractus Solitarii Following Hindlimb Unloading in Rats

Ludmila Lima-Silveira[a,c], **Diana Martinez**[a,c], **Eileen M. Hasser**[a,b,c], **David D. Kline**[a,c,*]

[a]Department of Biomedical Sciences, University of Missouri, 134 Research Park Dr., Columbia, MO 65211, USA

[b]Department of Medical Pharmacology and Physiology, University of Missouri, 134 Research Park Dr., Columbia, MO 65211, USA

[c]Dalton Cardiovascular Research Center, University of Missouri, 134 Research Park Dr., Columbia, MO 65211, USA

Abstract

Hindlimb unloading (HU) in rats induces cardiovascular deconditioning (CVD) analogous to that observed in individuals exposed to microgravity or bed rest. Among other physiological changes, HU rats exhibit autonomic imbalance and altered baroreflex function. Lack of change in visceral afferent activity that projects to the brainstem in HU rats suggests that neuronal plasticity within central nuclei processing cardiovascular afferents may be responsible for these changes in CVD and HU. The nucleus tractus solitarii (nTS) is a critical brainstem region for autonomic control and integration of cardiovascular reflexes. In this study, we used patch electrophysiology, live-cell calcium imaging and molecular methods to investigate the effects of HU on glutamatergic synaptic transmission and intrinsic properties of nTS neurons. HU increased the amplitude of monosynaptic excitatory postsynaptic currents and presynaptic calcium entry evoked by afferent tractus solitarii stimulus (TS-EPSC); spontaneous (s) EPSCs were unaffected. The addition of a NMDA receptor antagonist (AP5) reduced TS-EPSC amplitude and sEPSC frequency in HU but not control. Despite the increase in glutamatergic inputs, HU neurons were more hyperpolarized and exhibited intrinsic decreased excitability compared to controls. After block of ionotropic glutamatergic and GABAergic synaptic transmission (NBQX, AP5, Gabazine), HU neuronal membrane potential depolarized and neuronal excitability was comparable to controls. These data demonstrate that HU increases presynaptic release and TS-EPSC amplitude, which includes a NMDA receptor component. Furthermore, the decreased excitability and hyperpolarized membrane after HU are associated with enhanced GABAergic modulation. This functional neuroplasticity in the nTS may underly the CVD induced by HU.

*Correspondence to: David D. Kline, Department of Biomedical Sciences, University of Missouri, 134 Research Park Dr., Columbia, MO 65211, USA. klinedd@missouri.edu.

AUTHOR CONTRIBUTIONS

L.L.S, E.M.H., and D.D.K. designed the research; L.L.S, D.M. and DDK performed experiments and analyzed data; L.L.S, D.M, E.M.H., and D.D.K. interpreted results of experiments; L.L.S and D.D.K. prepared figures and drafted manuscript; L.L.S, D.M, E.M.H., and D.D.K. edited the manuscript and approved the final version.

CONFLICT OF INTEREST

The authors declare no competing financial interests.

Author Manuscript Author Manuscript Author Manuscript Author Manuscript

Keywords

glutamate; GABA; autonomic nervous system; cardiovascular deconditioning

INTRODUCTION

Individuals exposed to prolonged bed rest exhibit cardiovascular deconditioning (CVD) that is often associated with an imbalance of the sympathetic and parasympathetic nervous system (Taylor et al., 1949; Hasser and Moffitt, 2001; Hirayanagi et al., 2004). Similar dysautonomia is observed in rats exposed to hindlimb unloading (HU), a well-established model of CVD (Morey-Holton and Globus, 2002). Specifically, HU in rats induces vascular dysfunction and increased resting heart rate (Convertino et al., 1994; Delp et al., 1995; Moffitt et al., 1998, 2013; Mueller et al., 2005). HU also attenuates baroreflex-mediated sympathoexcitation to low blood pressure, the main regulator of cardiovascular responses to gravitational stress (Moffitt et al., 1998; Foley et al., 2005). The mechanisms by which CVD affects autonomic function and cardiovascular reflexes are not clear. Interestingly, we have shown that CVD does not alter baroreceptor afferent nerve activity (Moffitt et al., 1999), suggesting neuronal plasticity within central nuclei processing cardiovascular afferents are responsible for the dysfunction following CVD.

Visceral afferent fibers carrying cardiovascular information to the central nervous system establish their first synaptic contact with second-order neurons within the brainstem nucleus tractus solitarii (nTS) (Andresen and Kunze, 1994; Dampney, 1994; Andresen et al., 2004). nTS neurons integrate, process and modulate sensory information to ultimately activate downstream cardiovascular nuclei and reflexes, including the classical baroreflex pathway altered by HU (Dampney, 1994). Glutamate is the primary excitatory neurotransmitter released by sensory fibers onto nTS (Talman et al., 1980; Machado et al., 1997), while GABAergic inputs from interneurons or other brain regions represent the major inhibitory modulation to the neurons within this nucleus (Bailey et al., 2008). Thus, alteration in these signaling pathways may contribute to the CVD and HU effects on autonomic and cardiovascular function.

Previous studies have shown that synaptic plasticity in nTS neurotransmission contributes to several cardiovascular dysfunctions, including neurogenic hypertension, heart failure and high blood pressure following hypoxia (Kline, 2008; Zoccal et al., 2014; Lima-Silveira et al., 2019). Considering the critical role of nTS on autonomic control, in this study we investigated the effect of CVD following HU on glutamatergic neurotransmission and neuronal properties of nTS neurons. We hypothesized that HU increases glutamatergic modulation to the second-order nTS neurons, which could lead to the impaired baroreflex-mediated sympathoexcitation. In order to test this hypothesis, we combined whole-cell patch clamp recordings, live-cell calcium imaging and molecular analysis to evaluate several aspects of synaptic transmission and intrinsic properties of second-order nTS neurons. Our findings demonstrate HU increases the excitatory afferent-driven glutamatergic neurotransmission yet hyperpolarizes membrane potential and decreases neuronal

Author Manuscript Author Manuscript Author Manuscript Author Manuscript

excitability via enhanced GABAergic modulation. The increased synaptic transmission in HU is able to partially offset membrane hyperpolarization and induce action potential firing.

EXPERIMENTAL PROCEDURES

Animals

Three week-old male Sprague-Dawley rats (ENVIGO, Indianapolis, IN), were housed in individual cages with free access to water and food. The cages were maintained in an animal facility with controlled temperature (22 °C) and light–dark cycle 12:12-h. The experiments were conducted according to National Institutes of Health guidelines and all experimental protocols were previously approved by the Animal Care and Use Committees of the University of Missouri.

HU protocol

HU was induced as previously (Moffitt et al., 1998; Foley et al., 2005). Briefly, under isoflurane anesthesia (2%) stainless steel wire rings were placed in the proximal tail of HU and control rats. After a 1-week recovery, HU animals were acclimated to the unloading protocol by suspending the rats' hindlimbs via the attached rings at an angle of 30–35° for 1–3 h/day. Following 3 days of acclimation, the animals were tail suspended continuously for the next 14 days. A swivel suspension apparatus allowed the rats to move freely and have easy access to food and water. Control animals were maintained under normal postural conditions through the same period. The rats were monitored daily; rats that exhibited overt signs of stress or noticeable weight loss were excluded from the study.

nTS slice preparation and electrophysiology

After HU or control protocol, rats were deeply anesthetized with isoflurane and decapitated. The brainstem was quickly removed and placed in ice-cold artificial cerebrospinal fluid (aCSF) cutting solution containing the following: (in mM) 93 NMDG, 2.5 KCl, 1.2 NaH_2PO_4, 10 $MgSO_4$, 30 $NaHCO_3$, 20 HEPES, 25 D-glucose, 5 L-ascorbic acid, 2 thiourea, 3 sodium pyruvate and 0.5 $CaCl_2$. The pH of the solution was adjusted to 7.4 via ~93 mM HCl, osmolarity was 295–310 mosmol l^{-1}. The cutting NMDG-aCSF was constantly aerated with 95% O_2 + 5% CO_2 during the process of obtaining brainstem slices. A vibratome (VT 1000S or 1200, Leica, Wetzlar, Germany) was used to generate coronal brainstem slices (~260 μm) containing the nTS. Slices were incubated at 35 °C for 12 min in NMDG-cutting solution and then transferred to recording aCSF (in mM: 124 NaCl, 3 KCl, 1.2 NaH_2PO_4, 1.2 $MgSO_4$, 25 $NaHCO_3$, 11 D-glucose, 0.4 L-ascorbic acid and 2 $CaCl_2$, aerated with 95% O_2 + 5% CO_2, pH 7.4, 295–310 mosmol l^{-1}) where they were maintained for 30 + additional minutes at room temperature (~22 °C) until used.

Whole-cell patch-clamp recordings were performed similarly to previous published methods (Matott et al., 2016; Ostrowski et al., 2017). nTS slices were placed in a heated submerged recording chamber (TC-344B, Warner Instruments, Hamden, CT, USA) and superfused (~2.5 mL/min) with recording aCSF at ~32 °C continuously aerated with 95% O_2 + 5% CO_2. Viable neurons in the nTS region were visualized using a fixed stage upright microscope with DIC optics (BX51WI, Olympus, Japan). Pulled recording electrodes (Sutter

Author Manuscript Author Manuscript Author Manuscript Author Manuscript

B150-86) with a tip resistance (4–6 MΩ) were filled with a solution containing (in mM): 130 potassium gluconate, 10 NaCl, 11 EGTA, 10 HEPES, 1 $MgCl_2$, 1 $CaCl_2$, 2 MgATP and 0.2 NaGTP, pH 7.4, ~310 mosmol l^{-1}. After obtaining the whole-cell configuration the cells were held at a voltage (Vhold) of −60 mV for a stabilizing period of ~5 min. Cells with series resistance higher than 25 MΩ or that showed variation of ≥20% during the recordings were excluded from the analyses. Signals were filtered at 2 kHz and sampled at 10 kHz using a Multiclamp 700B amplifier (Molecular Devices, Sunnyvale, USA), connected to a data acquisition system (Digidata 1440, Molecular Devices, Sunnyvale, CA, USA) and recorded using the Clampex 10 software (Molecular Devices, Sunnyvale, USA).

Excitatory postsynaptic currents evoked by tractus solitarii stimulus (TS-EPSC) were recorded in voltage-clamp mode and held (V_{hold}) at −60 mV. A concentric bipolar electrode (FHC, Bowdoin, ME) was placed on afferent TS fibers which were stimulated at 0.5 Hz and 20 Hz. Resting membrane potential (RMP), spontaneous action potential (AP) discharge, and TS-evoked excitatory postsynaptic potentials (EPSPs) and Aps evoked at 20 Hz were recorded in current-clamp mode with no holding current (I=0). AP discharge was also evoked by depolarizing current steps (0–120 pA, 100 ms) or ramps (−20 to +100pA, 200 ms) in current clamp. In order to investigate the influence of the synaptic network on the RMP and excitability of neurons, the above-mentioned protocols were performed before and/or during pharmacological block of glutamatergic and GABAergic neurotransmission in some neurons.

Live-cell calcium imaging of visceral afferents

Visceral afferent fibers were prelabeled as described previously (Rogers et al., 2006; Martinez et al., 2020b). Briefly, two weeks preceding the beginning of the HU protocol, rats were anesthetized with isoflurane and a ventral midline incision in the neck was made to expose the nodose ganglion. The genetically encoded calcium indicator GCaMP6m (pAAV.Syn.GCaMP6m.WPRE.SV40, plasmid #100841, Addgene) was injected (~5 μL) into the ganglion with a Picospritzer (General Valve, Fairfield, NJ). The neck incision was closed with 4-0 Vicryl suture and antibiotic (Enrofloxacin 10 mg/kg, Newry, Northern Ireland, UK) and analgesic (Buprenorphine 0.05 mg/kg, Columbus, OH) were administered subcutaneously. Once recovered from anesthesia, the animals were individually placed in their home cage. Fourteen days following AAV injection rats were exposed to either HU or control as above. Fluorescence imaging were acquired after ~5 weeks of the virus injection, which allowed GCaMP6m to be expressed in the afferent terminals.

Horizontal nTS slices (250 μm) were generated similarly to that described above for electrophysiological experiments and positioned in a recording chamber. The slices were constantly perfused at a rate of 2.5 mL/min with aCSF (aerated with 95% O_2 + 5% CO_2) at a temperature of 33 °C. A bipolar electrode (FHC, Bowdoin, ME) was placed on the TS and a train of stimuli was applied (10 stimuli at 20 Hz). Time-lapse confocal calcium imaging were acquired via a Yokagawa CSU-W1 confocal system (3i, Denver, CO) using 40× water-immersion objective (Olympus ×40/0.8 W LUMPlanFL/IR), Prime 95B sCMOS camera (Photometrics), and a 488-nm excitation laser.

Author Manuscript Author Manuscript Author Manuscript Author Manuscript

Reverse transcription real-time polymerase chain reaction (RT-PCR) and immunoblots for NMDA receptors

RT-PCR was used to quantify the relative expression (Martinez et al., 2020a; Matott et al., 2020) of N-methyl-D-aspartate glutamate receptor (NMDAR) subunits (GluN1, GluN2A, GluN2B, GluN2C, GluN2D, GluN3A, GluN3B, Table 1). Control and HU rats were isoflurane anesthetized, decapitated and brainstem slices were generated. nTS region was separated, frozen in liquid nitrogen and stored at −80 °C. RNaquoeus-micro kit (Ambion: AM1931, Life Technologies, Grand Island, NY) was used to isolate mRNA from samples. 100 ng of mRNA was used to generate cDNA using oligo-dT primer set (Superscript III, Invitrogen: 18080-051). Next, quantitative RT-PCR from 2 μL of cDNA was executed using PowerUp SYBR Green master mix (Applied Biosystems), an Eppendorf Mastercycler system and primers for NMDAR subunits and the housekeeping gene β2-microglobulin (B2m, Table 1), all used at 10 μM; Fisher Scientific, Pittsburgh, PA). The amount of mRNA for each NMDAR subunit was normalized to B2m according to the $2^{-\Delta\Delta CT}$ method.

Protein expression of NR1 (subunit of NMDAR) and GluA1 (subunit of α-amino-3-hydroxy-5-methyl-4-isoxazo lepropionic acid glutamate receptor, AMPAR) was quantified via immunoblot (Martinez et al., 2020a; Matott et al., 2020). nTS tissue was obtained as described above and an extraction buffer (NP-40 1%, 150 mM NaCl, 50 mM Tris-HCl, 2.5 mM EDTA, protease inhibitors, Na-Deoxycholate 0.5%, SDS 0.1%) was used to homogenize the samples. The homogenate was centrifuged (15 min, 13,300 rpm, 4 °C) and the supernatant collected. Bio-Rad Protein Assay Dye Reagent (Bio-Rad, Hercules, CA, USA) was used to quantify protein concentration in the samples. 15 μg of protein was separated in a precast Mini-PROTEAN TGX gel (Bio-Rad) and then transferred to an Immun-Blot PVDF membrane (Bio-Rad). The pre-blocked membrane (5% powdered milk in Tris Buffered Saline containing 0.1% Tween 20) was incubated for 48 h with the primary antibody (NR1, 1:1000, Thermo-Fisher, Waltham, MA; or GluA1, 1 μg/mL, Abcam, Cambridge, MA) at 4 °C, washed and then incubated in the secondary antibody (1:20,000 NR1 and 1:10,000 GluA1, Jackson Immuno, West Grove, PA) for 2 h at room temperature. Mouse anti-tubulin (1:1000, Abcam, Cambridge, MA, RRID: AB_2241126) was used as the loading control antibody. The immunoblots were imaged using Bio-Rad ChemiDoc.

Pharmaceuticals

The antagonism of NMDA and non-NMDA glutamatergic receptors was accomplished by the addition of AP5 (10 μM) and NBQX (10 μM), respectively. Gabazine (GBZ, 25 μM) was used to antagonize $GABA_A$ receptors. Drugs were bath applied in a sequential and additive fashion. All the drugs were purchased from Tocris Bioscience (R&D Systems, Inc., Minneapolis, MN, USA).

Data analysis.

Electrophysiological data were analyzed off-line using Clampfit 10 (Molecular Devices) and Microsoft Excel software. Second-order nTS neurons were identified on the basis of the low standard deviation of the synaptic latency [i.e., jitter <300 μs (Ostrowski et al., 2014; Matott and Kline, 2016; Matott et al., 2017). Clampfit templates were used to detect EPSCs, with spontaneous (s) EPSC threshold set at 2× the root-mean-square noise level. TS-EPSC

Author Manuscript Author Manuscript Author Manuscript Author Manuscript

amplitude and the inverse of the squared coefficient of variation ($1/CV^2$) were evaluated from 20 replicates of the stimulus at 0.5 Hz. The average trace of TS-EPSC was normalized for the analysis of the rise time, decay time and half-width of the evoked events. Short-term depression was analyzed from five replicates of 10 consecutive stimulus at 20 Hz. sEPSCs were recorded for 2 min in gap-free mode without any stimulation. RMP and spontaneous AP discharge was recorded during 1 min with no holding current (I=0). The number of APs generated with TS stimulus, step-depolarization and AP rheobase were manually identified. Phase plot analysis (Jenerick, 1963) was used to determine the amplitude, hyperpolarizing after potential (HAP) and the threshold (dV/dt>11 mV/ms) of the first AP triggered by ramp protocol, all the other AP characteristics were generated via Clampfit. ImageJ (W.S. Rasband/National institute of Health, USA). Microsoft Excel were used to analyze the fluorescence [($\Delta F/F$)%] and area of GCaMP6m signals. For fluorescence analysis, 10 terminals with an evident fluorescent response to the TS stimulus were selected manually in each slice. From these 10 selected regions, the five that had the greatest response within each rat were used for the analysis. The area under the curve of fluorescence was calculated according to the trapezoidal rule. Immunoblots for NR1 and GluA1 were normalized to Tubulin expression.

Statistical analysis was performed with GraphPad Prism (version 7.0; GraphPad Software). Outliers were identified by Rout test and normality was evaluated using Shapiro–Wilk test. The differences between HU and control synaptic or neuronal properties were determined via Student's t test, Mann–Whitney test or ANOVA test where appropriate and noted in text. Results are expressed as dispersion of individual values±standard deviation (SD). Statistical significance was set at p<0.05.

RESULTS

HU increases afferent glutamatergic neurotransmission to second-order nTS neurons

Sensory afferent activity terminates onto single nTS neurons (Felder and Mifflin, 1988; Andresen and Yang, 1995; Doyle and Andresen, 2001). In order to evaluate the effects of HU on this excitatory monosynaptic input into the nTS, we stimulated the afferent fibers located within tractus solitarii (TS) and evaluated their evoked EPSCs (i.e., TS-EPSC). As shown in Fig. 1A, TS stimulation at 0.5 Hz evoked TS-EPSCs whose amplitude was greater in neurons from HU compared to controls. The significant increase in amplitude after HU is quantified in Fig. 1B (HU, n=15; control, n=11, Mann–Whitney test, p=0.0457). The augmented TS-EPSC amplitude after HU could be due to increased synaptic efficiency by presynaptic mechanisms and/or post-synaptic response to released glutamate. Therefore, we evaluated the variability of TS-EPSCs as an indicator of presynaptic release, and the kinetic properties of the TS-EPSC as indicators of postsynaptic glutamate receptor function. The squared coefficient of variation ($1/CV^2$) of 20 replicate evoked EPSCs was greater in neurons from HU rats compared to control animals (p=0.0228, Fig. 1C). By contrast, no changes were observed in the kinetic properties of the normalized TS-EPSC, as the rise time, decay time and half-width were comparable between groups (Fig. 1D-F). TS-EPSC amplitude of nTS cells that are polysynaptic (jitter >300 μs, i.e., higher-order) from visceral afferent fibers was comparable between groups (HU: 64±32 pA, n=7; control: 65±45 pA,

Author Manuscript Author Manuscript Author Manuscript Author Manuscript

n=8). Together, these data in monosynaptic neurons suggest that HU does not induce functional changes in postsynaptic glutamatergic receptor conductance, but rather HU enhances the presynaptic glutamate release on nTS neurons.

Baroafferent activity occurs as bursts of high frequency discharge with each heart beat (Andresen and Kunze, 1994; Andresen and Yang, 1995). Simulating this increased afferent activity by high frequency afferent stimulation (10 stimuli at 20 Hz) produced TS-EPSCs whose amplitude was greater in HU than controls and accommodated over time (Fig. 2A). The amplitude of the first TS-EPSC in second order nTS neurons was significantly greater in HU (*n*=15) than controls (*n*=10, Fig. 2B, $p=0.003$, two-way RM-ANOVA: stim, $p<0.0001$; HU, $p>0.05$; stim × HU, $p=0.0313$). Synaptic current amplitude decreased after the first initial event and was comparable between HU and controls. Normalizing TS-EPSC amplitude to the initial event demonstrated similar synaptic depression between HU and control (Fig. 2C). In addition to this synchronous release, the TS-nTS synapse possesses a high degree of asynchronous release that occurs following a repetitive stimulus train (Zhang and Mifflin, 2000; Kline et al., 2007; Kline, 2008; Peters et al., 2010). However, HU did not alter asynchronous EPSCs compared to controls (data not shown). Taken together, the data suggest that HU increased glutamate release but did not alter the rate of its depression from TS afferent fibers.

Calcium entry in TS terminals is increased by HU

Ca^{2+} entry into presynaptic afferents is a necessary step to induce neurotransmitter release (Katz and Miledi, 1967). As such, we determined if altered presynaptic Ca^{2+} mechanisms may be responsible for the enhanced TS-EPSC amplitude in monosynaptic neurons from HU-exposed rats. To do so, we examined the influx of calcium into pre-labeled GCaMP6M afferent terminals in response to 20 Hz TS stimulation (Kline et al., 2009; Martinez et al., 2020c). In response to TS stimulation, Ca^{2+} fluorescence increased in both groups but appeared greater in terminals from HU than controls (Fig. 3A); an example of the Ca^{2+} fluorescence over time is shown in Fig. 3B. The increase in fluorescence intensity in HU is illustrated by the significantly greater peak fluorescence $\Delta F/F\%$ (3 HU rats *n*=15 ROI, 4 control rats *n*=20 ROI, Fig. 3C, $p=0.0061$, Mann–Whitney test) and the tendency for greater elevation of fluorescence area (Fig. 3D, $p=0.0861$, Mann–Whitney test). These results indicate that an amplified calcium influx into TS afferents contributes to the increased glutamatergic neurotransmission in HU rats.

HU does not change the spontaneous release of glutamate through the network to second-order nTS neurons

nTS neurons receive multiple synaptic inputs from forebrain and medullary nuclei as well as from within the nTS itself (van der Kooy et al., 1984; Kawai and Senba, 1996). In order to evaluate the magnitude by which HU affects the neurotransmission within the nTS circuitry, we evaluated spontaneous (s) EPSCs in the absence of any stimulus. As shown in the representative examples (Fig. 4A), spontaneous synaptic currents in monosynaptically connected neurons were similar between HU and control rats. Neither sEPSC frequency (Fig. 4B) nor amplitude (Fig. 4C) was altered in HU animals (*n*=15) compared to control (*n*=11). These data indicate that the spontaneous glutamatergic neurotransmission to second-

Author Manuscript Author Manuscript Author Manuscript Author Manuscript

order nTS neurons is not affected by HU. However, nTS cells receiving indirect (polysynaptic) connections from afferent fibers had greater sEPSC frequency in HU compared to control as demonstrated in Fig. 4D and plotted in Fig. 4E (HU, n=6; control, n=8, p=0.0067 unpaired t-test). sEPSC amplitude was comparable in higher order neurons (Fig. 4F). The results show that the excitatory modulation from the network and/or nTS circuitry is increased on nTS neurons indirectly connected with afferent fibers after HU.

HU increases the contribution of NMDARs to neurotransmission

The visceral afferent integration into the nTS is primarily mediated by non-NMDA glutamate receptors (Andresen and Yang, 1990; Machado, 2001), with a smaller contribution of NMDA receptors (NMDAR). The contribution of NMDAR increases under certain physiological conditions, as in periods of augmented afferent activity (1999;; Seagard et al., 2003). We used the NMDAR antagonist AP5 (10 μM) to determine the extent HU may also enhance the role of these receptors in the augmented TS-EPSC amplitude in monosynaptic neurons. Representative traces in Fig. 5A demonstrate that AP5 did not alter TS-EPSC amplitude in cells from control rats whereas it substantially reduced current amplitude in HU-exposed rats. Moreover, the addition of a selective antagonist of non-NMDA receptors (NBQX, 10 μM) in the bath completely abolished TS-EPSCs in both groups and currents were not altered further by Gabazine (not shown). Averaged results are shown in Fig. 5B (HU, n=11; control, n=7, p=0.0179, paired t-test) demonstrating the reduction in TS-EPSC amplitude by AP5 in HU rats but not controls. In addition, during antagonism of NMDARs, synaptic depression produced by high frequency (20 Hz) TS-stimulation was more pronounced in HU compared to control (HU: n=11; Control: n=6, two-way RM-ANOVA: stim, p<0.0001; HU, p>0.05; stim × HU, p=0.0018) as exemplified in Fig. 5C and plotted in Fig. 5D.

Furthermore, we examined the effects of AP5 on sEPSCs in second-order nTS neurons. As shown in Fig. 5E, in the control group sEPSC frequency and amplitude were similar before and after AP5 (n=7). However, AP5 significantly reduced the frequency of sEPSCs in the HU neurons with no effect on amplitude. NBQX following AP5 eliminated all spontaneous events. Average data are shown in Fig. 5F and G and show that AP5 decreased sEPSC frequency in neurons from HU (n=11, p=0.0469, Wilcoxon matched-pairs signed rank test) but not controls (n=7); sEPSC amplitude was not altered in either group. The data suggest a greater contribution of NMDARs to excitatory neurotransmission in the nTS of HU rats.

The expression of NMDAR subunit mRNA and protein was examined in control and HU. The expression of the different NMDAR subunit transcripts was not altered in HU compared to control as shown in Fig. 6A. Similarly, the protein expression of NR1 and GluA1 was comparable between HU and control (Fig. 6B-D).

Hyperpolarization and decreased spontaneous and evoked firing activity after HU

Thus far we demonstrate HU increases monosynaptic synaptic transmission to second-order nTS neurons via a presynaptic mechanism as well as postsynaptic NMDAR component. These processes ultimately contribute to nTS activity; thus, the intrinsic membrane and discharge properties of second-order HU neurons were examined. Resting membrane

Author Manuscript Author Manuscript Author Manuscript Author Manuscript

potential (RMP) was hyperpolarized in HU neurons compared to control (Table 2). At RMP, 45% (5 of 11) of control neurons exhibited spontaneous action potentials (APs), while only 13% (2 of 16) of the HU cells showed spontaneous discharge (p=0.08, Fisher exact test). RMP of higher-order nTS neurons was similar between HU and controls (Control, −57±8, n=7; HU, −61±5, n=6).

A depolarizing ramp was utilized to evoke AP discharge for determination of the initial properties of second-order neurons (Fig. 7A). As shown in our representative examples, a greater amount of current (i.e., rheobase) was required to trigger an AP in HU compared to control. The mean data showing increased rheobase in HU (n=15) versus control (n=10) is shown in Fig. 7B (p=0.0132, unpaired t-test). Likewise, analysis of the first AP showed that HU shifted AP threshold in the depolarizing direction and decreased the AP amplitude, but had no effect on other AP properties (Table 2). Consistent with the reduced ability to generate an AP after HU, the voltage by which the cell needs to depolarize to fire an AP (RMP to THR) was greater in HU than control (Table 2).

To further explore the excitability of second-order nTS neurons after HU, we quantified the evoked AP discharge generated with current step-depolarization. Fig. 7C shows AP discharge evoked by 120 pA in both groups. The representative traces demonstrate that HU had decreased firing activity compared to control. Indeed, HU reduced the overall number of evoked action potentials with increasing current amplitude, as quantified in Fig. 7D (HU: n=16; Control: n=11, two-way RM-ANOVA: current (pA), p<0.0001; HU, p=0.0004; current (pA) × HU, p<0.0001). By contrast, excitability of nTS neurons polysynaptically connected to sensory afferents was similar between controls and HU (APs triggered by 120 pA: CC: 3.4±1.9, n=7; HU: 4.8±2.4, n=6). Altogether, the results indicate HU changes intrinsic characteristics of second-order but not higher-order nTS neurons which ultimately lead to decreased neuronal firing rate in second-order neurons.

Reduced firing rate following HU is modulated by synaptic inputs on nTS neurons

The neuronal membrane potential and firing frequency can be influenced by changes in their intrinsic properties and/or the synaptic inputs they receive. Pharmacological blockade of glutamatergic excitatory and GABAergic inhibitory neurotransmission (NBQX 10 μM; AP5 10 μM; Gabazine (GBZ) 25 μM) in second-order nTS neurons was used to assess their influence on membrane potential and AP discharge after HU. Progressive and complete synaptic transmission blockade had no effect on the RMP of control rats (n=6, Fig. 8A). By contrast, complete synaptic blockade significantly depolarized RMP from HU neurons (n=7, Fig. 8A, one-way RM-ANOVA test: ACSF × synaptic blockade, p=0.0474), under this condition, RMP from HU neurons was comparable to control Furthermore, during synaptic transmission blockade, the number of APs generated via step-depolarization was not different between control and HU (Fig. 8B, HU: n=7; control: n=6). These findings indicate that hyperpolarized RMP and reduced excitability of second-order nTS neurons following HU are dependent on synaptic modulation.

Author Manuscript Author Manuscript Author Manuscript Author Manuscript

AP discharge induced by TS stimulation is unaltered in HU neurons

The data described above shows that HU increases TS-EPSC amplitude yet reduces the excitability of second-order nTS neurons. To investigate the effect of the increased excitatory neurotransmission on the firing activity of nTS neurons, we evaluated the action potential discharge induced by high frequency (20 Hz) nTS stimulus. As illustrated in Fig. 9A, the number of APs induced by TS-stimulus was similar between HU and control neurons (Fig. 9B, HU n=6, control: n=5). This result indicates that the increased glutamatergic afferent-driven (TS-EPSC) transmission in second-order nTS neurons is sufficient to compensate the hyperpolarization of nTS neurons from HU animals thus producing similar AP discharge between HU and controls.

DISCUSSION

Dysautonomia and impaired baroreflex are major contributors to orthostatic intolerance and reduced exercise capacity following CVD (Convertino et al., 1982, 1990; Eckberg and Fritsch, 1992; Fritsch-Yelle et al., 1994; Woodman et al., 1995). We have shown the HU rat model mimics many of the CVD manifestations, including impaired baroreflex, but also enhances cardiopulmonary reflexes and plasma vasopressin (Moffitt et al., 1998, 2008; Hasser and Moffitt, 2001; Mueller et al., 2006b). Our studies further suggested that alterations in central regions processing viscerosensory signaling may mediate impaired reflex signaling (Moffitt et al., 1999). The nTS is the first central site where autonomic and cardiovascular reflex function are integrated. Thus, in the present study, we used the HU rat model to investigate the effects of CVD on excitatory glutamatergic neurotransmission and neuronal properties of nTS neurons. We show that HU significantly modified synaptic transmission and neuronal excitability in neurons directly (second-order) connected with visceral afferents. In these neurons, HU enhanced TS-evoked EPSC amplitude yet reduced their excitability. By contrast, TS-EPSC amplitude and neuronal excitability were not altered in higher-order neurons while spontaneous excitatory current frequency was augmented. Our results demonstrate, for the first time, HU induces pathway specific synaptic plasticity and neuronal activity within the nTS region.

Sensory afferent synaptic transmission to second-order nTS neurons is glutamatergic (Talman et al., 1980; Andresen and Yang, 1990) and characterized by its high fidelity and release probability, and low failure rate (Andresen and Yang, 1995; Doyle and Andresen, 2001; Kline et al., 2007). These second-order neurons directly project to many autonomic nervous system nuclei, including the rostral and caudal ventrolateral medulla (RVLM, CVLM) and to a lesser extent the paraventricular nucleus of the hypothalamus (PVN) (Andresen and Kunze, 1994; Affleck et al., 2012; Lima-Silveira et al., 2019), regions that have been implicated in HU alterations (Moffitt et al., 2002; Mueller et al., 2003, 2006a). Therefore, alterations in monosynaptic visceral afferent-nTS soma neurotransmission may directly modify neuronal function and ultimately autonomic modulation of the cardiovascular system (Zhang and Mifflin, 2000; Kline et al., 2007; Kline, 2008). We show that low frequency afferent (TS) stimulation produces larger amplitude TS-EPSCs in second-order nTS neurons after HU than control. A similar increase in TS-EPSC amplitude was seen during the initial events within a 20 Hz stimulus train, while synaptic

Author Manuscript Author Manuscript Author Manuscript Author Manuscript

accommodation within the train was similar between groups. This increase in current amplitude could be attributed to a greater release of glutamate by afferent fibers, and/or an exaggerated response of postsynaptic neurons. Several lines of evidence suggest both pre- and postsynaptic mechanisms may contribute.

We initially evaluated the synaptic variability ($1/CV^2$) of TS-EPSCs, a parameter that is sensitive to presynaptic changes (Malinow and Tsien, 1990) and an indicator of presynaptic plasticity in nTS (Kline et al., 2007; Almado et al., 2012; Lima-Silveira et al., 2019; Matott et al., 2020). HU increased $1/CV^2$ compared to control, suggesting presynaptic alterations in release probability and/or the number of functional synapses (Bekkers and Stevens, 1990; Malinow and Tsien, 1990). HU also significantly enhanced afferent terminal GCaMP6m Ca^{2+} fluorescence intensity in response to TS stimulation, further indicating presynaptic modification of release by HU. Calcium entry through voltage-gated Ca^{2+} channels is a requisite for synchronous neurotransmitter release and its plasticity (Mendelowitz and Kunze, 1992; Catterall and Few, 2008). Whether this increase in presynaptic Ca^{2+} and resulting evoked EPSCs in HU is due to alteration of the voltage-gated Ca^{2+} channel subtype responsible for glutamate release [in nTS N-type, but also P/Q-, L- or T-type channels, (Mendelowitz and Kunze, 1992; Mendelowitz et al., 1995)], the presynaptic Ca^{2+} sensor or Ca^{2+} regulatory proteins (Catterall and Few, 2008) requires further study. Last, TS-EPSC rise, decay and half-width were comparable between HU and controls, suggesting the enhancement of TS-EPSC amplitude in HU was not attributed to augmented glutamate binding or postsynaptic glutamatergic receptor sensitivity. Altogether, these data suggest that HU-enhanced TS-evoked glutamatergic neurotransmission occurs via Ca^{2+} dependent presynaptic plasticity.

In addition to the evidence for enhanced presynaptic release, HU also increased the contribution of the NMDA receptors in second-order neurons. Glutamate release from visceral afferent fibers binds primarily to non-NMDA receptors on second-order nTS neurons (Andresen and Yang, 1990). However, in vitro and in vivo studies have shown that both non-NMDA and NMDA receptors contribute to the integration of cardiovascular reflexes and EPSCs in the nTS (Haibara et al., 1995; Aylwin et al., 1997). It has been demonstrated that NMDA receptors play a critical role in the fidelity of neurotransmission during high frequency afferent discharge (Zhao et al., 2015). Indeed, the contribution of NMDA receptors to TS-nTS neurotransmission may increase under elevated levels of excitatory-afferent driven activity, including baroafferent activity (Bonham and Chen, 2002; Seagard et al., 2003), which may be attributed to the membrane depolarization that is required to release NMDA receptors from voltage-dependent Mg^{2+} block (Nowak et al., 1984). Our data revealed a greater role of NMDA receptors to excitatory neurotransmission following HU. The NMDAR antagonist AP5 significantly reduced TS-EPSC amplitude in HU neurons to that of controls. Moreover, in the presence of AP5, the synaptic depression induced by high frequency TS-stimulation was greater in HU than control, which further suggested increased contribution of NMDARs to the excitatory throughput in HU. Regardless, the greater NMDAR contribution in HU is likely not due to increased receptor expression, as neither NMDAR subunits transcripts nor NR1 protein were increased after HU compared to controls. The GluA1 subunit for AMPA receptors was also comparable. Expression analysis was performed on the entire nTS region, which includes second- and

Author Manuscript Author Manuscript Author Manuscript Author Manuscript

high-order neurons but also non-neuronal cell types. Therefore, the possible selective effect of HU on NMDAR expression in second-order nTS neurons remains under consideration. Consistent with the primary role of non-NMDA receptors in TS-EPSCs, the antagonism of non-NMDAR by NBQX was efficient at abolishing all synaptic currents in both groups (Andresen and Yang, 1990).

In addition to sensory information, nTS neurons receive synaptic inputs from multiple CNS regions, including cortical, forebrain, brainstem sites as well as interneurons within the nTS circuit. These inputs regulate both tonic and phasic activity of postsynaptic neurons (van der Kooy et al., 1984; Andresen and Kunze, 1994; Kawai and Senba, 1996). Unlike TS-EPSCs from HU rats, the frequency and amplitude of spontaneous events (sEPSC) were similar in second-order neurons to those in control. However, block of NMDARs with AP5 reduced the frequency of sEPSCs in HU-exposed neurons but not in controls, further confirming an elevated contribution of NMDARs in HU. The primary effect of NMDAR block on sEPSC frequency but not amplitude in HU likely indicates these receptors are located, and perhaps enhanced, on the presynaptic terminal or its soma that innervates the recorded neuron (Yen et al., 1999).

Postsynaptic nTS neuron activity is modulated by the balance of excitatory and inhibitory inputs that converge onto these neurons (Champagnat et al., 1986; Dekin and Getting, 1987; Andresen and Kunze, 1994). Despite our results showing that HU increased excitatory inputs on second-order nTS neurons, these cells were more hyperpolarized and had reduced excitability compared to their control. The reduced excitability after HU was demonstrated by the higher rheobase; increased AP threshold and decreased amplitude and AP discharge in response to depolarizing currents. The reduced AP amplitude may suggest a reduction in voltage-gated sodium channels expression or function that may contribute to reduced excitability. By contrast, AP rise, decay and after hyperpolarization were comparable between groups. The capacitance and input resistance were comparable between the groups, which indicates that decreased neuronal excitability in HU was not related to alterations in somal size or electrical compactness.

We investigated the role of the synaptic network in the hyperpolarized RMP and reduced firing rate of second-order nTS neurons via synaptic block of excitatory and inhibitory neurotransmission. Neither glutamatergic nor GABAergic receptor blockade altered RMP or discharge of control neurons. In HU rats, while RMP and discharge were not affected by blockade of NMDAR or non-NMDAR, antagonism of GABAergic signaling significantly depolarized neurons. HU firing rate was also comparable to controls after complete blockade. These findings indicate that HU neurons are under more inhibitory modulation. However, the greater excitatory drive from the visceral afferents seems to counterbalance this inhibition, since the TS stimulus produces comparable AP discharge between HU and control. The extent that HU alters ion channel expression or function to influence membrane potential or firing remains to be examined.

Although the sensory modality or phenotype of the recorded monosynaptic neurons is not known, they exhibit distinct responses from those of higher-order neurons. Specifically, TS-EPSC amplitude in higher-order neurons was similar between the groups. HU also had no

Author Manuscript Author Manuscript Author Manuscript Author Manuscript

effect on neuronal excitability (AP, rheobase, or threshold) in these neurons. Interestingly, the frequency of sEPSC increased in higher-order nTS neurons in HU animals. The increased glutamate release onto higher-order neurons may shift the membrane potential toward the action potential threshold, which could facilitate the nTS processing of inputs from several different reflex pathways [e.g., chemoreflex (Accorsi-Mendonça and Machado, 2013) or cardiopulmonary (Dampney, 1994; Mueller and Hasser, 2003)] or other physiological functions which were otherwise affected by HU. The increased FosB expression in nTS of HU rats (Hollenbeck et al., 2003) is consistent with the potential for greater activity in these polysynaptic neurons. Altogether, HU induces selective effects on distinct nTS neuronal subgroups.

As noted earlier, alterations in nTS neurons activity may affect multiple pathways involved in neural control of cardiovascular function. The hyperpolarization and reduced excitability of second-order nTS neurons from HU rats could be correlated with the increased resting heart rate via decreased excitatory modulation of nTS to nucleus ambiguous or CVLM, and increased circulating vasopressin by reduction of the indirect inhibition from nTS neurons to vasopressinergic hypothalamic nuclei (Moffitt et al., 1998; Mueller et al., 2006b). The increased GABAergic inhibition after HU may also limit the ability of the nTS to further reduce its activity upon baroreceptor unloading and subsequently attenuate sympathoexcitation. Otherwise, the increased glutamatergic neurotransmission on second-order (evoked EPSCs) and higher-order (spontaneous EPSCs) nTS neurons from HU is consistent with data showing enhanced cardiopulmonary reflex and impaired sympathetic-excitatory mediated baroreflex in HU exposed rats (Moffitt et al., 1998; Mueller et al., 2006b). The precise mechanisms by which HU alters the central pathways involved in autonomic control remain under investigation. Indeed, future studies are necessary to investigate the electrophysiological characteristics of distinct populations of nTS neurons integrating the different cardiovascular and respiratory reflexes. Moreover, it might be relevant to evaluate the time course of alterations in glutamatergic and GABAergic neurotransmission in nTS during HU protocol. It is possible that the increase in GABAergic modulation observed in HU may serve to compensate the enhanced excitatory drive and thus avoid the hyperactivation of nTS neurons.

In summary, in this study we combined several technical approaches to investigate the synaptic transmission and electrophysiological characteristics of nTS neurons from HU-exposed rats. Our results show that HU induces synaptic and neuronal plasticity in nTS neurons mono- and polysynaptically connected with TS. These results strongly support the concept that alterations in the nTS may contribute to the basal autonomic and reflex effects of CVD following HU.

ACKNOWLEDGEMENTS

This study was supported by NIH HL132836 (EMH) and HL128454 (DDK) & American Autonomic Society-Lundbeck Fellowship (LLS). We thank Sarah Friskey and Colbren Trogstad-Isaacson for the technical support in Hindlimb Unloading protocol and Heather Dantzler and Katherine Langen for their technical expertise in immunoblots and PCR.

Author Manuscript Author Manuscript Author Manuscript Author Manuscript

Abbreviations:

AP	action potential
CVD	cardiovascular deconditioning
HU	Hindlimb unloading
nTS	nucleus tractus solitarii
RMP	Resting membrane potential

REFERENCES

Accorsi-Mendonça D, Machado BH (2013) Synaptic transmission of baro- and chemoreceptors afferents in the NTS second order neurons. Auton Neurosci 175:3–8. [PubMed: 23305891]

Affleck VS, Coote JH, Pyner S (2012) The projection and synaptic organisation of NTS afferent connections with presympathetic neurons, GABA and nNOS neurons in the paraventricular nucleus of the hypothalamus. Neuroscience 219:48–61. [PubMed: 22698695]

Almado CE, Machado BH, Leão RM (2012) Chronic intermittent hypoxia depresses afferent neurotransmission in NTS neurons by a reduction in the number of active synapses. J Neurosci 32:16736–16746. [PubMed: 23175827]

Andresen MC, Doyle MW, Bailey TW, Jin YH (2004) Differentiation of autonomic reflex control begins with cellular mechanisms at the first synapse within the nucleus tractus solitarius. Braz J Med Biol Res 37:549–558. [PubMed: 15064818]

Andresen MC, Kunze DL (1994) Nucleus tractus solitarius–gateway to neural circulatory control. Annu Rev Physiol 56:93–116. [PubMed: 7912060]

Andresen MC, Yang M (1995) Dynamics of sensory afferent synaptic transmission in aortic baroreceptor regions on nucleus tractus solitarius. J Neurophysiol 74:1518–1528. [PubMed: 8989390]

Andresen MC, Yang MY (1990) Non-NMDA receptors mediate sensory afferent synaptic transmission in medial nucleus tractus solitarius. Am J Physiol 259:H1307–H1311. [PubMed: 1977326]

Aylwin ML, Horowitz JM, Bonham AC (1997) NMDA receptors contribute to primary visceral afferent transmission in the nucleus of the solitary tract. J Neurophysiol 77:2539–2548. [PubMed: 9163375]

Bailey TW, Appleyard SM, Jin YH, Andresen MC (2008) Organization and properties of GABAergic neurons in solitary tract nucleus (NTS). J Neurophysiol 99:1712–1722. [PubMed: 18272881]

Bekkers JM, Stevens CF (1990) Presynaptic mechanism for long-term potentiation in the hippocampus. Nature 346:724–729. [PubMed: 2167454]

Bonham AC, Chen CY (2002) Glutamatergic neural transmission in the nucleus tractus solitarius: N-methyl-D-aspartate receptors. Clin Exp Pharmacol Physiol 29:497–502. [PubMed: 12010198]

Catterall WA, Few AP (2008) Calcium channel regulation and presynaptic plasticity. Neuron 59:882–901. [PubMed: 18817729]

Champagnat J, Jacquin T, Richter DW (1986) Voltage-dependent currents in neurones of the nuclei of the solitary tract of rat brainstem slices. Pflugers Arch 406:372–379. [PubMed: 2423952]

Convertino V, Hung J, Goldwater D, DeBusk RF (1982) Cardiovascular responses to exercise in middle-aged men after 10 days of bedrest. Circulation 65:134–140. [PubMed: 6796287]

Convertino VA, Doerr DF, Eckberg DL, Fritsch JM, Vernikos-Danellis J (1990) Head-down bed rest impairs vagal baroreflex responses and provokes orthostatic hypotension. J Appl Physiol (1985) 68:1458–1464. [PubMed: 2347788]

Convertino VA, Doerr DF, Ludwig DA, Vernikos J (1994) Effect of simulated microgravity on cardiopulmonary baroreflex control of forearm vascular resistance. Am J Physiol 266:R1962–R1969. [PubMed: 8024053]

Author Manuscript Author Manuscript Author Manuscript Author Manuscript

Dampney RA (1994) Functional organization of central pathways regulating the cardiovascular system. Physiol Rev 74:323–364. [PubMed: 8171117]

Dekin MS, Getting PA (1987) In vitro characterization of neurons in the ventral part of the nucleus tractus solitarius. II. Ionic basis for repetitive firing patterns. J Neurophysiol 58:215–229. [PubMed: 2441002]

Delp MD, Brown M, Laughlin MH, Hasser EM (1995) Rat aortic vasoreactivity is altered by old age and hindlimb unloading. J Appl Physiol (1985) 78:2079–2086. [PubMed: 7665402]

Doyle MW, Andresen MC (2001) Reliability of monosynaptic sensory transmission in brain stem neurons in vitro. J Neurophysiol 85:2213–2223. [PubMed: 11353036]

Eckberg DL, Fritsch JM (1992) Influence of ten-day head-down bedrest on human carotid baroreceptor-cardiac reflex function. Acta Physiol Scand Suppl 604:69–76. [PubMed: 1509895]

Felder RB, Mifflin SW (1988) Modulation of carotid sinus afferent input to nucleus tractus solitarius by parabrachial nucleus stimulation. Circ Res 63:35–49. [PubMed: 3383382]

Foley CM, Mueller PJ, Hasser EM, Heesch CM (2005) Hindlimb unloading and female gender attenuate baroreflex-mediated sympathoexcitation. Am J Physiol Regul Integr Comp Physiol 289:R1440–R1447. [PubMed: 16051718]

Fritsch-Yelle JM, Charles JB, Jones MM, Beightol LA, Eckberg DL (1994) Spaceflight alters autonomic regulation of arterial pressure in humans. J Appl Physiol (1985) 77:1776–1783. [PubMed: 7836199]

Haibara AS, Colombari E, Chianca DA Jr, Bonagamba LG, Machado BH (1995) NMDA receptors in NTS are involved in bradycardic but not in pressor response of chemoreflex. Am J Physiol 269: H1421–H1427. [PubMed: 7485576]

Hasser EM, Moffitt JA (2001) Regulation of sympathetic nervous system function after cardiovascular deconditioning. Ann N Y Acad Sci 940:454–468. [PubMed: 11458701]

Hirayanagi K, Iwase S, Kamiya A, Sasaki T, Mano T, Yajima K (2004) Functional changes in autonomic nervous system and baroreceptor reflex induced by 14 days of 6 degrees head-down bed rest. Eur J Appl Physiol 92:160–167. [PubMed: 15042373]

Jenerick H (1963) Phase Plane Trajectories Of The Muscle Spike Potential. Biophys J 3:363–377. [PubMed: 14062456]

Katz B, Miledi R (1967) Ionic requirements of synaptic transmitter release. Nature 215:651. [PubMed: 4292912]

Kawai Y, Senba E (1996) Organization of excitatory and inhibitory local networks in the caudal nucleus of tractus solitarius of rats revealed in in vitro slice preparation. J Comp Neurol 373:309–321. [PubMed: 8889930]

Kline DD (2008) Plasticity in glutamatergic NTS neurotransmission. Respir Physiol Neurobiol 164:105–111. [PubMed: 18524694]

Kline DD, Hendricks G, Hermann G, Rogers RC, Kunze DL (2009) Dopamine inhibits N-type channels in visceral afferents to reduce synaptic transmitter release under normoxic and chronic intermittent hypoxic conditions. J Neurophysiol 101:2270–2278. [PubMed: 19244351]

Kline DD, Ramirez-Navarro A, Kunze DL (2007) Adaptive depression in synaptic transmission in the nucleus of the solitary tract after in vivo chronic intermittent hypoxia: evidence for homeostatic plasticity. J Neurosci 27:4663–4673. [PubMed: 17460079]

Lima-Silveira L, Accorsi-Mendonca D, Bonagamba LGH, Almado CEL, da Silva MP, Nedoboy PE, Pilowsky PM, Machado BH (2019) Enhancement of excitatory transmission in NTS neurons projecting to ventral medulla of rats exposed to sustained hypoxia is blunted by minocycline. J Physiol 597:2903–2923. [PubMed: 30993693]

Machado BH (2001) Neurotransmission of the cardiovascular reflexes in the nucleus tractus solitarii of awake rats. Ann N Y Acad Sci 940:179–196. [PubMed: 11458676]

Machado BH, Mauad H, Chianca Junior DA, Haibara AS, Colombari E (1997) Autonomic processing of the cardiovascular reflexes in the nucleus tractus solitarii. Braz J Med Biol Res 30:533–543. [PubMed: 9251775]

Malinow R, Tsien RW (1990) Presynaptic enhancement shown by whole-cell recordings of long-term potentiation in hippocampal slices. Nature 346:177–180. [PubMed: 2164158]

Author Manuscript Author Manuscript Author Manuscript Author Manuscript

Martinez D, Rogers RC, Hasser EM, Hermann GE, Kline DD (2020a) Loss of excitatory amino acid transporter restraint following chronic intermittent hypoxia contribute to synaptic alterations in nucleus tractus solitarii. J Neurophysiol.

Martinez D, Rogers RC, Hasser EM, Hermann GE, Kline DD (2020b) Loss of excitatory amino acid transporter restraint following chronic intermittent hypoxia contributes to synaptic alterations in nucleus tractus solitarii. J Neurophysiol 123:2122–2135. [PubMed: 32347148]

Martinez D, Rogers RC, Hermann GE, Hasser EM, Kline DD (2020c) Astrocytic glutamate transporters reduce the neuronal and physiological influence of metabotropic glutamate receptors in nucleus tractus solitarii. Am J Physiol Regul Integr Comp Physiol 318:R545–R564. [PubMed: 31967862]

Matott MP, Hasser EM, Kline DD (2020) Sustained hypoxia alters nTS glutamatergic signaling and expression and function of excitatory amino acid transporters. Neuroscience 430:131–140. [PubMed: 32032667]

Matott MP, Kline DD (2016) Activation of 5-hyrdoxytryptamine 7 receptors within the rat nucleus tractus solitarii modulates synaptic properties. Brain Res 1635:12–26. [PubMed: 26779891]

Matott MP, Kline DD, Hasser EM (2017) Glial EAAT2 regulation of extracellular nTS glutamate critically controls neuronal activity and cardiorespiratory reflexes. J Physiol 595:6045–6063. [PubMed: 28677303]

Matott MP, Ruyle BC, Hasser EM, Kline DD (2016) Excitatory amino acid transporters tonically restrain nTS synaptic and neuronal activity to modulate cardiorespiratory function. J Neurophysiol 115:1691–1702. [PubMed: 26719090]

Mendelowitz D, Kunze DL (1992) Characterization of calcium currents in aortic baroreceptor neurons. J Neurophysiol 68:509–517. [PubMed: 1326604]

Mendelowitz D, Reynolds PJ, Andresen MC (1995) Heterogeneous functional expression of calcium channels at sensory and synaptic regions in nodose neurons. J Neurophysiol 73:872–875. [PubMed: 7760142]

Moffitt JA, Foley CM, Schadt JC, Laughlin MH, Hasser EM (1998) Attenuated baroreflex control of sympathetic nerve activity after cardiovascular deconditioning in rats. Am J Physiol 274: R1397–R1405. [PubMed: 9612408]

Moffitt JA, Grippo AJ, Beltz TG, Johnson AK (2008) Hindlimb unloading elicits anhedonia and sympathovagal imbalance. J Appl Physiol (1985) 105:1049–1059. [PubMed: 18635876]

Moffitt JA, Heesch CM, Hasser EM (2002) Increased GABA(A) inhibition of the RVLM after hindlimb unloading in rats. Am J Physiol Regul Integr Comp Physiol 283:R604–R614. [PubMed: 12184994]

Moffitt JA, Henry MK, Welliver KC, Jepson AJ, Garnett ER (2013) Hindlimb unloading results in increased predisposition to cardiac arrhythmias and alters left ventricular connexin 43 expression. Am J Physiol Regul Integr Comp Physiol 304:R362–R373. [PubMed: 23302960]

Moffitt JA, Schadt JC, Hasser EM (1999) Altered central nervous system processing of baroreceptor input following hindlimb unloading in rats. Am J Physiol 277:H2272–H2279. [PubMed: 10600846]

Morey-Holton ER, Globus RK (2002) Hindlimb unloading rodent model: technical aspects. J Appl Physiol (1985) 92(1367).

Mueller PJ, Cunningham JT, Patel KP, Hasser EM (2003) Proposed role of the paraventricular nucleus in cardiovascular deconditioning. Acta Physiol Scand 177:27–35. [PubMed: 12492776]

Mueller PJ, Foley CM, Hasser EM (2005) Hindlimb unloading alters nitric oxide and autonomic control of resting arterial pressure in conscious rats. Am J Physiol Regul Integr Comp Physiol 289: R140–R147. [PubMed: 15761183]

Mueller PJ, Foley CM, Heesch CM, Cunningham JT, Zheng H, Patel KP, Hasser EM (2006a) Increased nitric oxide synthase activity and expression in the hypothalamus of hindlimb unloaded rats. Brain Res 1115:65–74. [PubMed: 16938283]

Mueller PJ, Hasser EM (2003) Enhanced sympathoinhibitory response to volume expansion in conscious hindlimb-unloaded rats. J Appl Physiol (1985) 94:1806–1812. [PubMed: 12533501]

Author Manuscript Author Manuscript Author Manuscript Author Manuscript

Mueller PJ, Sullivan MJ, Grindstaff RR, Cunningham JT, Hasser EM (2006b) Regulation of plasma vasopressin and renin activity in conscious hindlimb-unloaded rats. Am J Physiol Regul Integr Comp Physiol 291:R46–R52. [PubMed: 16469838]

Nowak L, Bregestovski P, Ascher P, Herbet A, Prochiantz A (1984) Magnesium gates glutamate-activated channels in mouse central neurones. Nature 307:462–465. [PubMed: 6320006]

Ostrowski TD, Dantzler HA, Polo-Parada L, Kline DD (2017) H2O2 augments cytosolic calcium in nucleus tractus solitarii neurons via multiple voltage-gated calcium channels. Am J Physiol Cell Physiol 312:C651–C662. [PubMed: 28274920]

Ostrowski TD, Ostrowski D, Hasser EM, Kline DD (2014) Depressed GABA and glutamate synaptic signaling by 5-HT1A receptors in the nucleus tractus solitarii and their role in cardiorespiratory function. J Neurophysiol 111:2493–2504. [PubMed: 24671532]

Peters JH, McDougall SJ, Fawley JA, Smith SM, Andresen MC (2010) Primary afferent activation of thermosensitive TRPV1 triggers asynchronous glutamate release at central neurons. Neuron 65:657–669. [PubMed: 20223201]

Rogers RC, Nasse JS, Hermann GE (2006) Live-cell imaging methods for the study of vagal afferents within the nucleus of the solitary tract. J Neurosci Methods 150:47–58. [PubMed: 16099514]

Seagard JL, Dean C, Hopp FA (2003) Activity-dependent role of NMDA receptors in transmission of cardiac mechanoreceptor input to the NTS. Am J Physiol Heart Circ Physiol 284:H884–H891. [PubMed: 12578816]

Seagard JL, Dean C, Hopp FA (1999) Role of glutamate receptors in transmission of vagal cardiac input to neurones in the nucleus tractus solitarii in dogs. J Physiol 520(Pt 1):243–253. [PubMed: 10517815]

Talman WT, Perrone MH, Reis DJ (1980) Evidence for L-glutamate as the neurotransmitter of baroreceptor afferent nerve fibers. Science 209:813–815. [PubMed: 6105709]

Taylor HL, Henschel A, et al. (1949) Effects of bed rest on cardiovascular function and work performance. J Appl Physiol 2:223–239. [PubMed: 15398582]

van der Kooy D, Koda LY, McGinty JF, Gerfen CR, Bloom FE (1984) The organization of projections from the cortex, amygdala, and hypothalamus to the nucleus of the solitary tract in rat. J Comp Neurol 224:1–24. [PubMed: 6715573]

Woodman CR, Sebastian LA, Tipton CM (1995) Influence of simulated microgravity on cardiac output and blood flow distribution during exercise. J Appl Physiol (1985) 79:1762–1768. [PubMed: 8594039]

Yen JC, Chan JY, Chan SH (1999) Differential roles of NMDA and non-NMDA receptors in synaptic responses of neurons in nucleus tractus solitarii of the rat. J Neurophysiol 81:3034–3043. [PubMed: 10368418]

Zhang J, Mifflin SW (2000) Integration of aortic nerve inputs in hypertensive rats. Hypertension 35:430–436. [PubMed: 10642337]

Zhao H, Peters JH, Zhu M, Page SJ, Ritter RC, Appleyard SM (2015) Frequency-dependent facilitation of synaptic throughput via postsynaptic NMDA receptors in the nucleus of the solitary tract. J Physiol 593:111–125. [PubMed: 25281729]

Zoccal DB, Furuya WI, Bassi M, Colombari DS, Colombari E (2014) The nucleus of the solitary tract and the coordination of respiratory and sympathetic activities. Front Physiol 5:238. [PubMed: 25009507]

Author Manuscript Author Manuscript Author Manuscript Author Manuscript

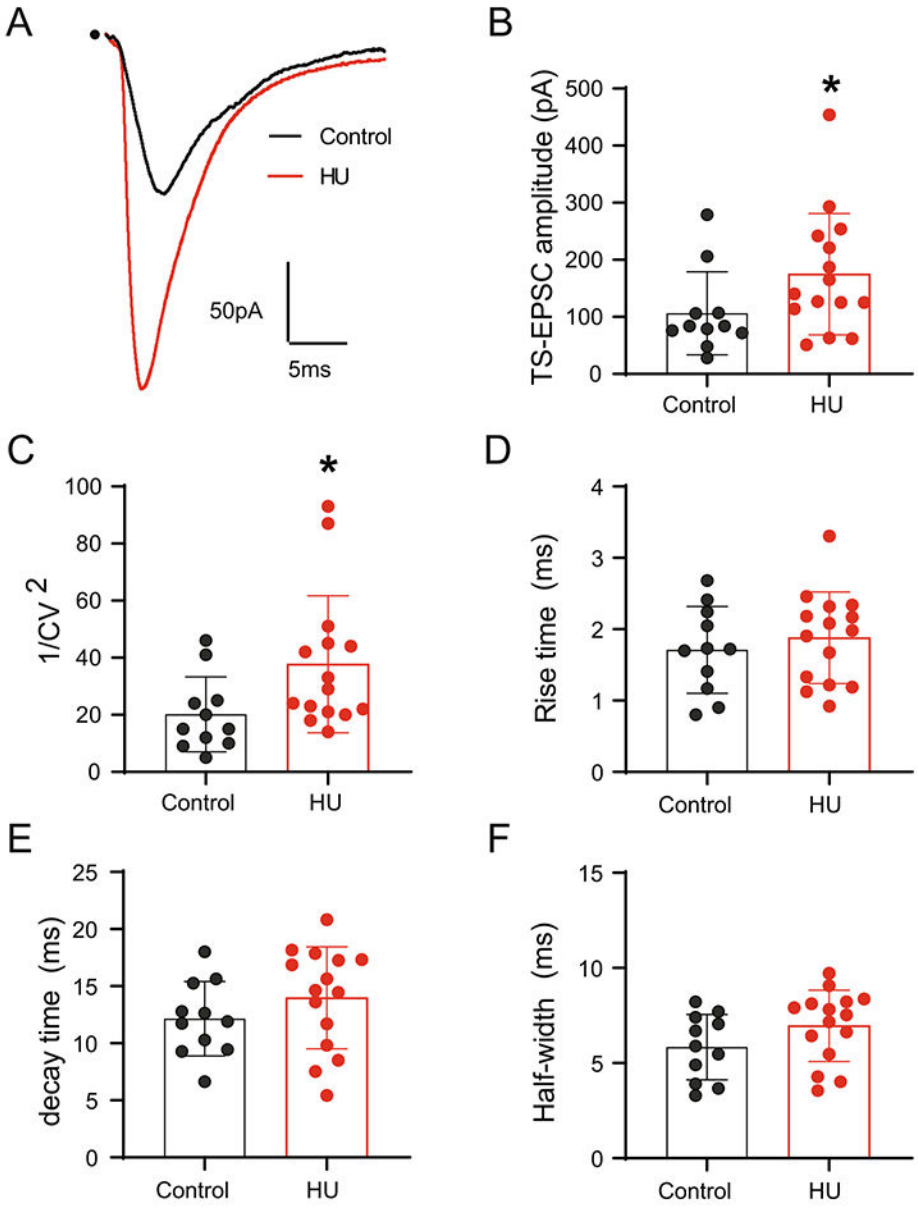

Fig. 1.

HU increases TS-EPSC amplitude in second-order nTS neurons. **(A)** Example traces of TS-EPSCs in second-order nTS neurons from a control (black) and HU (red) rat, dot indicates the point of stimulus. Shown is the average of 20 individual TS-EPSCs of each neuron. Note the increase in the amplitude in HU rat. **(B)** Average data of TS-EPSC amplitude showing an enhanced glutamatergic neurotransmission in neurons from HU rats. **(C)** Quantification of squared coefficient of variation ($1/CV^2$), the increase in this parameter indicates presynaptic plasticity in HU rats. **(D–F)** HU does not alter TS-EPSC rise time **(D)**, decay time **(E)** and half width **(F)** compared to controls. Data are shown as mean±SD. *p<0.05 HU *vs* control, Mann–Whitney test.

Author Manuscript Author Manuscript Author Manuscript Author Manuscript

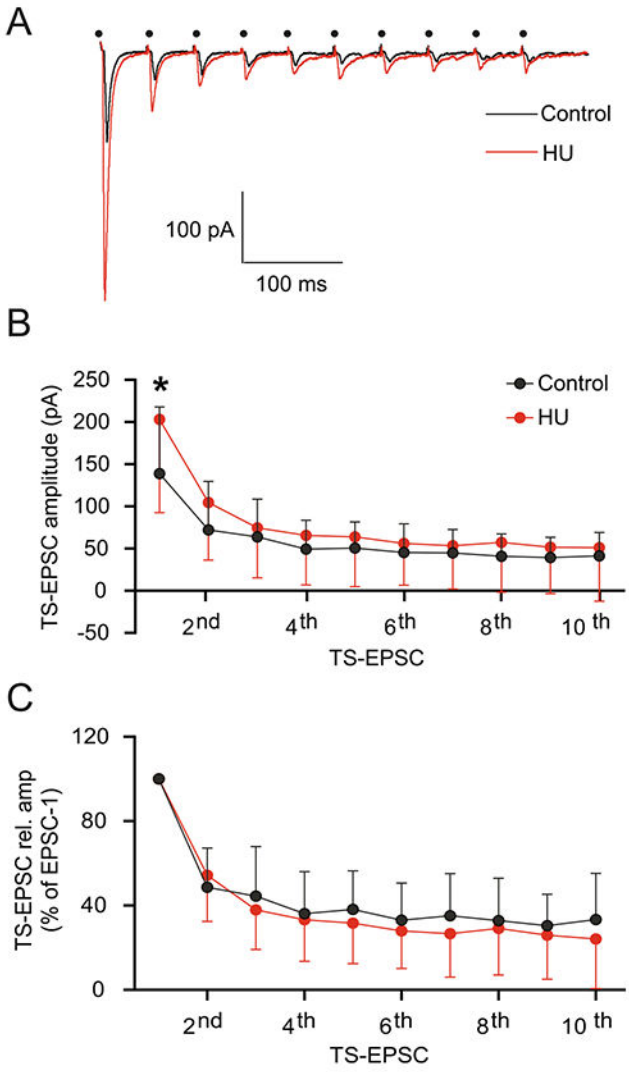

Fig. 2.

Short-term depression of TS-EPSC is not affected by HU. **(A)** Representative traces of TS-EPSC from a control (black) and HU (red) neuron during consecutive 20 Hz stimulation, dot indicates the point of stimulus. Although HU TS-EPSC amplitude was initially greater, short-term depression in nTS synapses occurred as in control. **(B)** Average data showing the synaptic depression in both control and HU group. The amplitude of the first TS-EPSC is greater in HU, yet the amplitude of subsequent events was comparable between control and HU groups. **(C)** Normalizing TS-EPSC amplitude to the first event showing comparable synaptic depression between control and HU. Data are shown as mean±SD. *p<0.05 HU *vs* control, two-way ANOVA with Fisher's LSD test.

Author Manuscript Author Manuscript Author Manuscript Author Manuscript

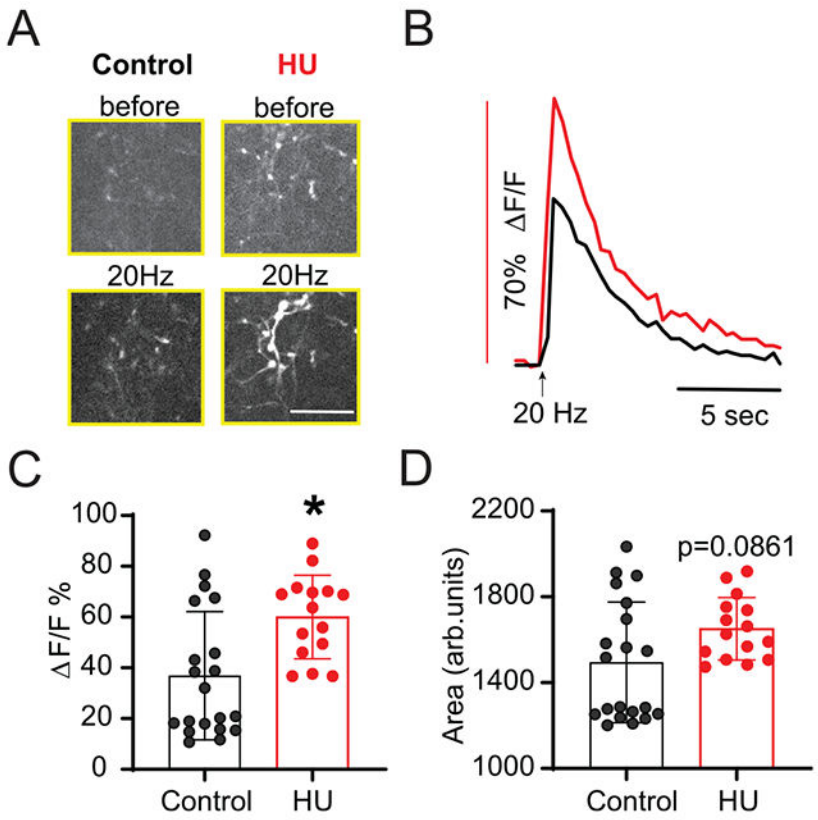

Fig. 3.

HU increases TS-afferent calcium entry. **(A)** Live-cell calcium imaging demonstrating individual afferent (GCaMP6m pre-labeled) before and during TS stimulation at 20 Hz (scale bar: 30 μm). Calcium influx following TS stimuli is greater in HU compared to control. **(B)** Example traces of Ca^{2+} fluorescence from a control (black) and HU (red) afferent during TS stimuli showing that the magnitude of fluorescence response is increased in HU. **(C)** Average changes in fluorescence reported as percent change from pre-stimulation base-line (Δ*F*/*F*%). **(D)** Quantitative data of fluorescence area showing the near significant increase in HU compared to control. Data are shown as mean±SD. *p<0.05 HU *vs* control, Mann–Whitney test **(C, D)**.

Author Manuscript Author Manuscript Author Manuscript Author Manuscript

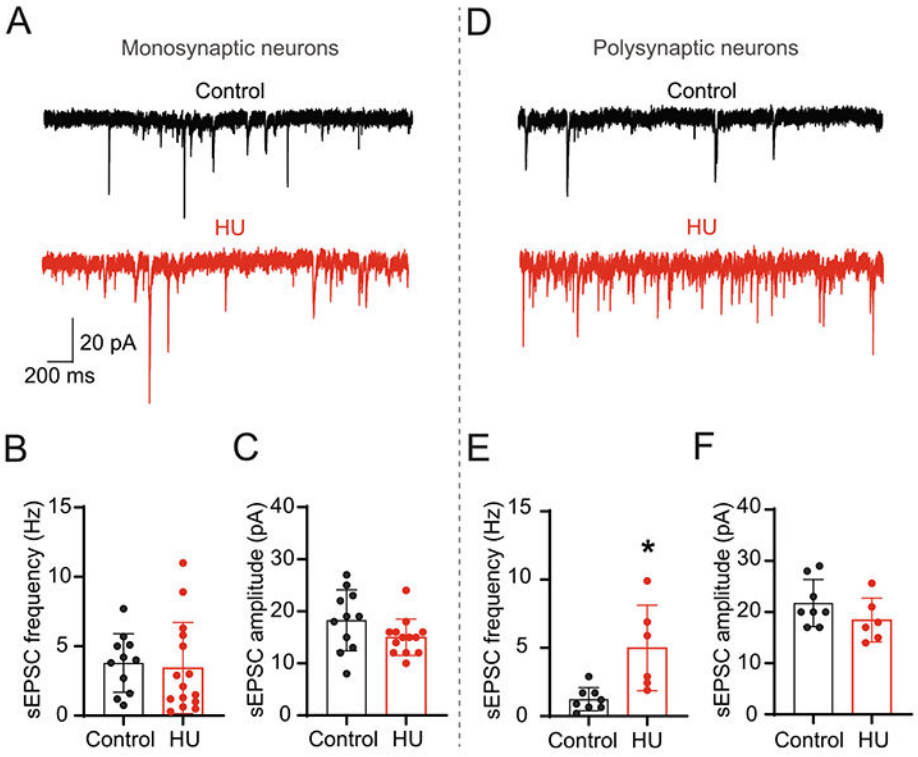

Fig. 4.

HU increases spontaneous EPSCs in nTS neurons polysynaptically connected to sensory afferents but not in second-order nTS neurons. **(A)** Representative recording of comparable sEPSCs in second-order nTS neurons from a control (black) and HU (red) rat. **(B, C)** Mean data of sEPSC frequency **(B)** and amplitude **(C)** of both experimental groups. **(D)** Representative examples of sEPSCs from a control (black) and HU (red) neuron indirectly (polysynaptic) connected with TS afferents. Note the higher frequency of sEPSC in HU. **(E, F)** Quantitative data of frequency **(E)** and amplitude **(F)** of sEPSC in nTS neurons polysynaptically connected (higher-order) with visceral afferents. Data are shown as mean ±SD. *p<0.05 HU *vs* control, unpaired t-test.

Author Manuscript Author Manuscript Author Manuscript Author Manuscript

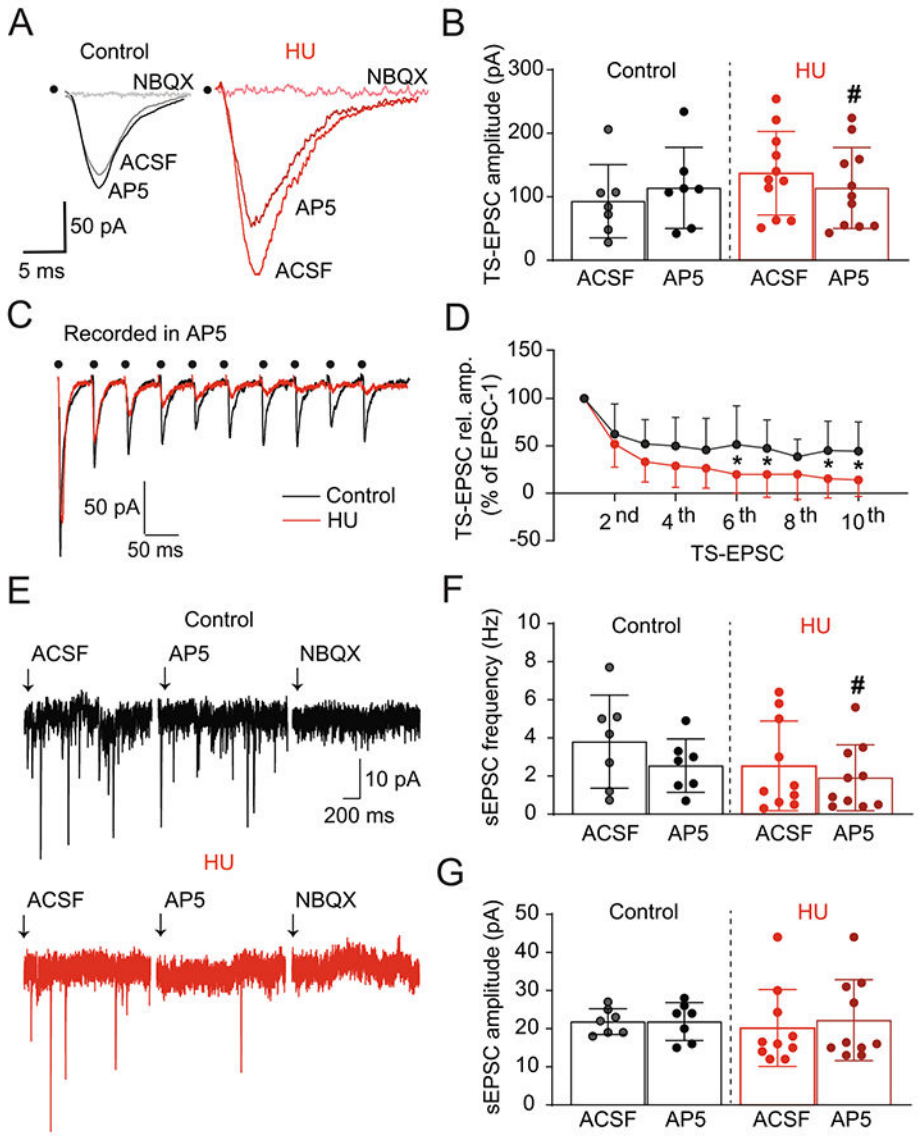

Fig. 5.

HU enhances NMDAR-mediated neurotransmission in second-order neurons. **(A)** Representative traces of TS-EPSCs from a control (black) and HU (red) rat before and after the selective antagonism of NMDAR (AP5, 10 μM) and non-NMDAR (NBQX, 10 μM). AP5 had no effect on control neurons, yet it substantially reduced current amplitude in HU cells. NBQX completely abolished TS-EPSCs in both groups. **(B)** Average data of TS-EPSC amplitude before and after AP5, indicating the participation of NMDA receptors in the increased glutamatergic neurotransmission in HU neurons. **(C)** Example recordings demonstrating TS-EPSCs during AP5 and the greater effect of AP5 on short-term synaptic depression of TS-EPSCs in HU (red) compared to control (black), dot indicates the point of stimulus. **(D)** Average data of TS-EPSC amplitude normalized to the first event after 10 stimuli at 20 Hz. **(E)** Example recordings showing the effects of NMDAR and non-NMDAR blockade on sEPSCs from a control (black) and HU (red) rat. In control neurons, frequency and amplitude of sEPSCs were unaffected by AP5, whereas it substantially reduced the

Author Manuscript Author Manuscript Author Manuscript Author Manuscript

frequency of events in HU-exposed rats. NBQX eliminated all spontaneous events in control and HU. Mean data showing the effect of AP5 on sEPSC frequency and amplitude of both groups are plotted in **(F)** and **(G)**, respectively. *p<0.05 control *vs* HU two-way RM-ANOVA, $^{\#}p$<0.05 AP5 *vs* ACSF, paired *t*-test **(B)** and Wilcoxon matched-pairs signed rank test **(F)**.

Author Manuscript Author Manuscript Author Manuscript Author Manuscript

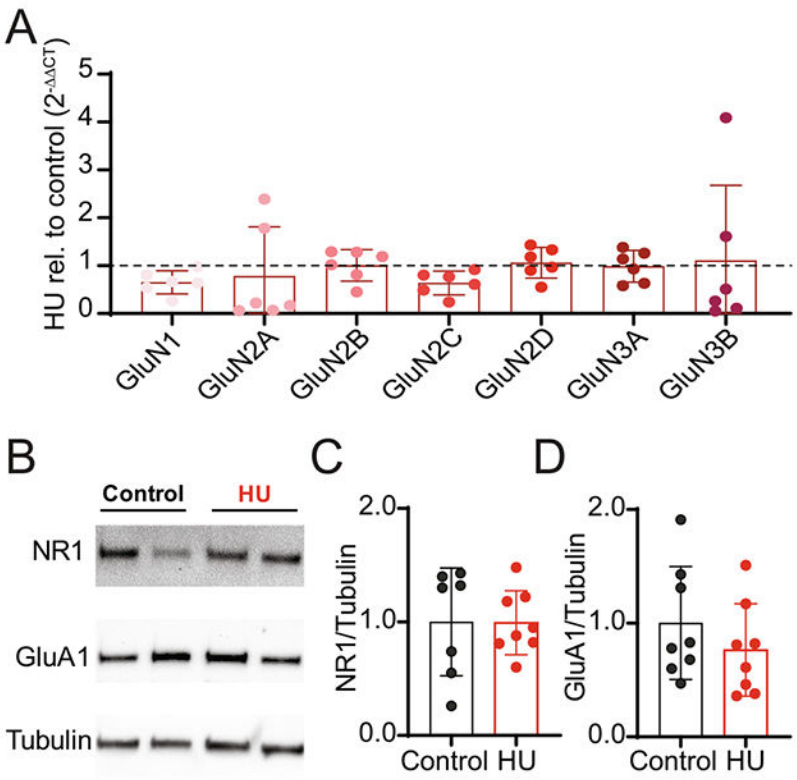

Fig. 6.

HU does not change mRNA and protein expression of glutamatergic receptors. **(A)** mRNA expression of NMDAR subunits (GluN1, GluN2A, GluN2B, GluN2C, GluN2D, GluN3A, GluN3B) relative to *B2m*. Values are normalized to control rats ("1", represented by dashed line). **(B)** Representative immunoblot for NR1, GluA1 and tubulin of two control and two HU individual nTS samples. **(C, D)** Quantification of NR1 and GluA1 protein expression, relative to tubulin, in the nTS of control and HU rat. Values are normalized to control rats ("1"). Data are shown as mean±SD.

Author Manuscript Author Manuscript Author Manuscript Author Manuscript

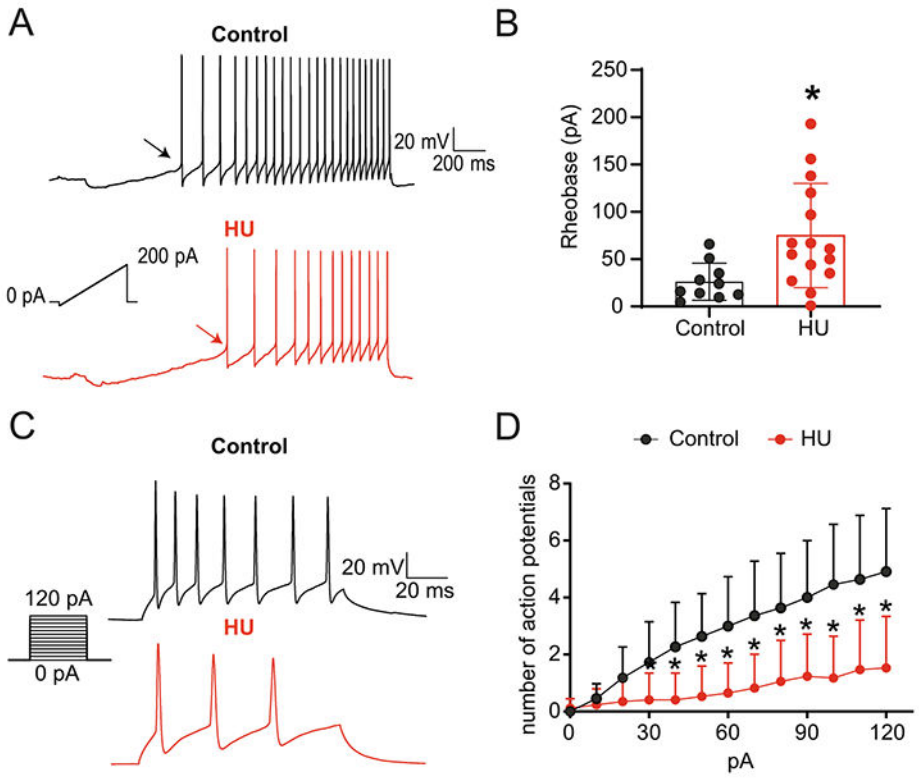

Fig. 7.

Decreased excitability of second-order nTS neurons following HU. **(A)** Representative recordings of AP discharge evoked by injection of depolarizing current (ramp) in nTS neurons from a control (black) and HU (red) rat. Arrows indicate the Rheobase of each neuron. Note more current needed to induce AP in HU rat. **(B)** Average data showing the increased Rheobase in HU compared to control. **(C)** Recordings of AP discharge in response to step-depolarization. The representative traces show APs triggered by the higher-amplitude current (120 pA). **(D)** Quantification of AP discharge triggered by each depolarizing current amplitude injected into nTS neurons demonstrating the reduced number of APs in neurons of HU rats. *p<0.05 HU *vs* control, unpaired *t*-test **(B)** two-way ANOVA with Fisher's LSD test **(D)**.

Author Manuscript Author Manuscript Author Manuscript Author Manuscript

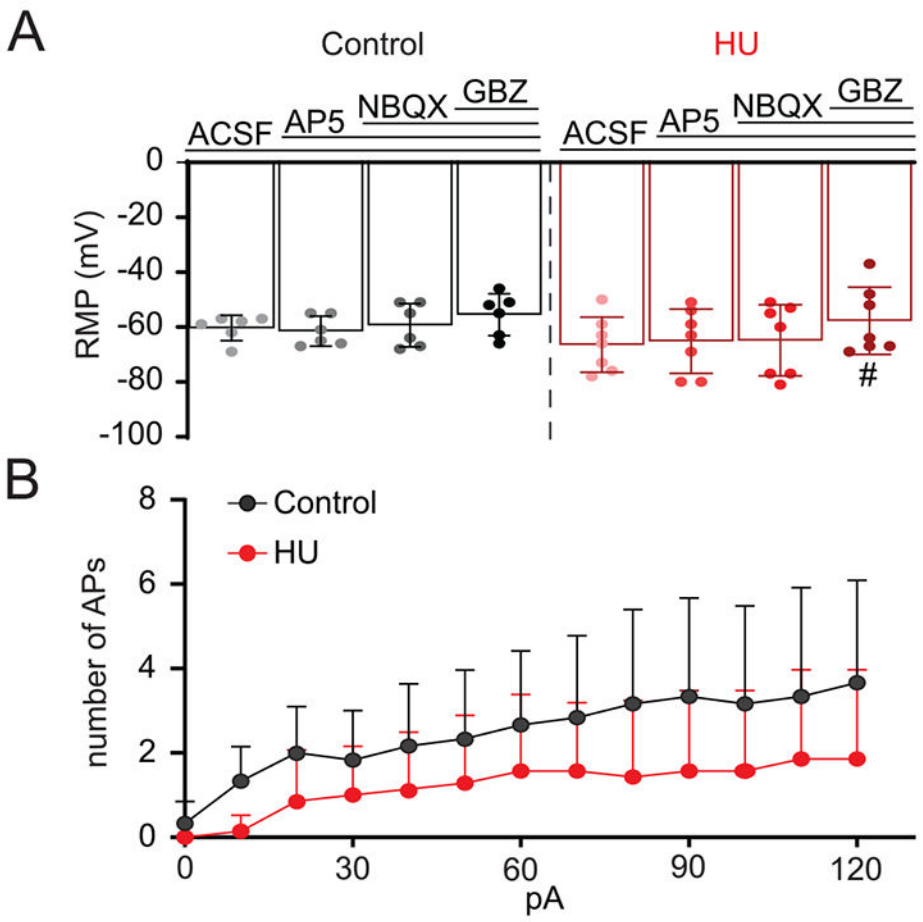

Fig. 8.

Hyperpolarization of HU membrane potential is mediated by inhibitory synaptic inputs on second-order nTS neurons. **(A)** Mean data showing the effects of progressive neurotransmission blockade (AP5 10 μM; NBQX 10 μM; GBZ 25 mM) on RMP of control (black) and HU (red) group. Synaptic blockade produced no changes in RMP of control cells. By contrast, whereas RMP of HU neurons was not affected by glutamatergic receptors blockade, antagonism of GABAergic neurotransmission (GBZ) significantly depolarized these cells. **(B)** Average data illustrating the number of action potentials evoked by step-depolarization after complete synaptic blockade. Note that under this condition, the firing rate is comparable between control and HU. $^{\#}p<0.05$ Gabazine *vs* ACSF, one-way RM-ANOVA test.

Author Manuscript Author Manuscript Author Manuscript Author Manuscript

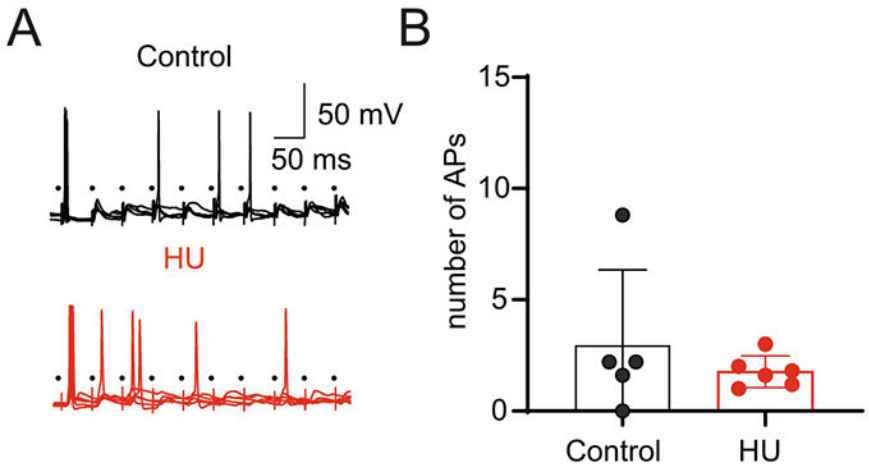

Fig. 9.

HU afferent synaptic plasticity maintains AP discharge evoked by TS stimulation. **(A)** Example recordings showing APs induced by TS-stimulation (5 sweeps, 10 times at 20 Hz) in a neuron from control (black) and HU (red). Only a single trace is shown for representative purposes. **(B)** Average data showing the comparable number of evoked APs in control and HU.

Author Manuscript Author Manuscript Author Manuscript Author Manuscript

Table 1.

Primers for NMDAR subunits

Primer	Sequence	
	Forward	Reverse
GluN1 NM_017010	gcttttgcagccgtgaac	gggctctgctctaccactctt
GluN2A NM_012573	ccaccttctccggctacag	gcaataccagcaaggtccag
GluN2B NM_012574	catggtatctcgcagcaatg	cagcgctgaatggctctaa
GluN2C NM_012575	ctggcactcctgcaacttct	ttctggcagatccctgagag
GluN2D NM_012575	gcagcaatggcactgtgt	cgaacatcatcacccagaca
GluN3A NM_138546	aagagaagctttgccgtcac	caacagcacgaagagtccag
GluN3B NM_133308	ttccagttacacggccaac	agcgaaagccttgggaag
B2m NM_012512	agcaggttcctcaaacaa gg	ttctgccttggagtcctttc

Neuroscience. Author manuscript; available in PMC 2021 November 21.

Author Manuscript Author Manuscript Author Manuscript Author Manuscript

Table 2.

Intrinsic properties: control vs HU. Values are mean ± SD of the intrinsic membrane properties and action potential (AP) characteristics of second-order nTS neurons from control and HU rats. HAP, afterpolarization. Ri, input resistance. AP amplitude and HAP values determined from

	Control (mean±SD)	HU (mean±SD)	*p* value (control vs HU)
RMP (mV)	− 58±8	− 65±7	0.0377*
AP Threshold (mV)	− 36±8	−25±11	0.0171*
Threshold-RMP (mV)	23±9	40±13	0.0029*
AP Amplitude (mV)	75±10	58±13	0.0024*
AP HAP (mV)	−21±5	−25±7	>0.05
AP Half Width (ms)	0.89±0.35	1±0.48	>0.05
AP Rise Time (ms)	0.31±0.10	0.42±0.23	>0.05
AP Decay Time (ms)	0.61±0.29	0.65±0.36	>0.05
Capacitance (pF)	20±7	23±7	>0.05
Ri (MΩ)	734±447	579±341	>0.05

Neuroscience. Author manuscript; available in PMC 2021 November 21.